# Hollow shell–corona microspheres with a mesoporous shell as potential microreactors for Au-catalyzed aerobic oxidation of alcohols†

**Li Yang, Minchao Zhang, Yang Lan and Wangqing Zhang***

***Received (in Victoria, Australia) 30th December 2009, Accepted 2nd March 2010***
***First published as an Advance Article on the web 28th April 2010***
**DOI: 10.1039/b9nj00802k**

Au-functionalized hollow shell–corona microspheres with a mesoporous shell are proposed as a microreactor for aerobic alcohol oxidation. These microreactors are constructed by template polymerization followed by hydrolysis of the shell-forming polyvinyltriethoxylsilane segment, and contain a hydrophilic corona to keep the microreactors suspended in the aqueous phase and a mesoporous chelate shell to immobilize Au nanoparticles and to increase the permeability of the microreactors. These microreactors have the ability to encapsulate and concentrate reactants, and have been demonstrated to mediate Au-catalyzed aerobic alcohol oxidation, which takes place efficiently in a quasi-homogeneous aqueous solution and under organic–aqueous biphasic conditions, since the reactants are highly concentrated within the microcavity. Other benefits of the microreactors include easy catalyst reuse, low catalyst leaching and long-term stability.



## 1. Introduction

Recently, tailor-made micro- or nanoreactors have been of growing interest to chemists, as they provide a confined environment within which chemical conversion can take place efficiently (due to the concentrated reactants) and/or selectively (due to its specific reaction sites).[1,2] Up to now, lots of reactors, varying in size from a few nanometers to tens of micrometers, including inorganic ones such as yolk–shell catalytic nanoreactors,[3–5] and organic or polymeric ones such as vesicles[6–8] and hollow spheres,[9–11] have been fabricated to provide a confined microenvironment within which conversion takes place efficiently and selectively. Generally, micro- or nanoreactors should possess three characteristics:[12] (1) fast diffusion of both reactants and products through the shell or wall; (2) a suitable structure to restrict the catalytic species; (3) an acceptable long-term stability.

Poor permeability is the key limitation for micro- or nanoreactors (such as polymersomes) because the thick wall or shell hinders the movement of reactants and products. Two strategies have been usually used to overcome this limitation. The first is to incorporate proton pumps in the polymersome membrane.[13] The second is to incorporate channels across the thick shell through which regulation of the flux of molecules in and out of the microenvironment is made. For example, Meier's group has developed a permeable ABA triblock copolymer polymersome nanoreactor by incorporating the OmpF channel protein in the membrane.[12] These channels therefore allow direct access to enzymes encapsulated within the interior of these vesicles.

In a recent communication, we proposed a microreactor of Pd nanoparticles immobilized hollow shell–corona microspheres of poly[styrene-*co*-2-(acetoacetoxy)ethyl methacrylate-*co*-acrylamide] (PS-*co*-PAEMA-*co*-PAM) for olefin hydrogenation under organic–aqueous biphasic conditions.[14] Herein, in order to increase the permeability of microreactor, hollow shell–corona microspheres with a mesoporous shell of poly[styrene-*co*-2-(acetoacetoxy)ethyl methacrylate-*co*-ethylene-*co*-methylacrylic acid] (PS-*co*-PAEMA-*co*-PE-*co*-PMAA) are synthesized and the microreactor with Au nanoparticles immobilized within it is tested for aerobic alcohol oxidation. This proposed microreactor, as shown in Fig. 1, is composed of three parts: (1) the hydrophilic corona of poly(methacrylic acid) (PMAA); (2) the crosslinked, chelating, mesoporous shell of poly[styrene-*co*-2-(acetoacetoxy)-ethyl methacrylate-*co*-ethylene] (PS-*co*-PAEMA-*co*-PE); and (3) Au nanoparticles embedded in the mesoporous shell. It is found that this microreactor is efficient for aerobic alcohol oxidation in quasi-homogeneous aqueous solution or under organic–aqueous biphase condition.

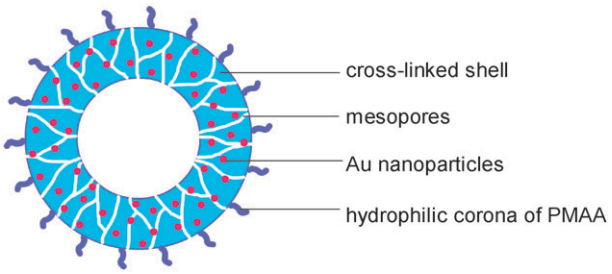


**Fig. 1** Structure of the microreactor.

*Key Laboratory of Functional Polymer Materials of Ministry of Education, Institute of Polymer Chemistry, Nankai University, Tianjin 300071, China. E-mail: wqzhang@nankai.edu.cn; Fax: +86-22-23503510; Tel: +86-22-23509794*
† Electronic supplementary information (ESI) available: Additional experimental information. See DOI: 10.1039/b9nj00802k

## 2. Experimental

### 2.1 Materials

Styrene (St, >98%) and methylacrylic acid (MAA, >99%) were purchased from Tianjin Chemical Company and distilled under vacuum before being used. Divinylbenzene (DVB, >80%, Alfa Aesar) was washed with 5% NaOH aqueous solution and water, followed by drying with $MgSO_4$. The monomers, 2-(acetoacetoxy)ethyl methacrylate (AEMA, >95%, Aldrich) and vinyltriethoxysilane (VTES, >95%, Tianjin Chemical Company), $K_2S_2O_8$ (>99.5%, Tianjin Chemical Company), $HAuCl_4{\cdot}3H_2O$ (>99.9%, Tianjin Chemical Company), $NaBH_4$ (>98.9%, Tianjin Chemical Company), 1-phenylethanol (>99%, Alfa Aesar), 1-(4-methoxyphenyl)ethanol (>95%, Alfa Aesar), 1-(4-methylphenyl)ethanol (>98%, Acros), 1-(2-methylphenyl)ethanol (>98%, Alfa Aesar), 1-(4-chlorophenyl)ethanol (>97%, Alfa Aesar), benzyl alcohol (>99%, Tianjin Chemical Company) and benzhydrol (>99%, Alfa Aesar), were used as received.

### 2.2 Synthesis of the microspheres

**2.2.1 Preparation of the core template of PS-*co*-PMAA microspheres.** The core template of poly(styrene-*co*-methylacrylic acid) (PS-*co*-PMAA) microspheres was synthesized as described elsewhere.[15] To a flask, MAA (0.430 g, 5.0 mmol) was first dissolved in 100 mL water to form a homogeneous solution. Subsequently, styrene (5.208 g, 50.0 mmol) was added. The mixture was degassed with nitrogen at room temperature, and then $K_2S_2O_8$ (0.297 g, 1.1 mmol) was added. The mixture was degassed again, and polymerization was performed with vigorous stirring at 80 °C for 24 h under a nitrogen atmosphere. Then the product of the PS-*co*-PMAA microspheres was purified by centrifugation and washed thrice with water. The product of PS-*co*-PMAA microspheres was dispersed in 150.0 mL of water for subsequent use.

**2.2.2 Preparation of the PS-*co*-PAEMA-*co*-PVTES-*co*-PMAA hollow microspheres.** The hollow microspheres of poly[styrene-*co*-2-(acetoacetoxy)ethyl methacrylate-*co*-vinyltriethoxylsilane-*co*-methylacrylic acid] (PS-*co*-PAEMA-*co*-PVTES-*co*-PMAA) were synthesized by template polymerization.[16,17] To a flask, 0.135 g of $K_2S_2O_8$ was added to 45.0 mL of the aqueous dispersion of the PS-*co*-PMAA microspheres (containing 1.69 g of the PS-*co*-PMAA microspheres). The mixture was firstly degassed with nitrogen at room temperature for 30 min with vigorous stirring. Subsequently, the mixture was heated to 80 °C, and then the mixture of styrene (1.043 g, 10.0 mmol), AEMA (1.071 g, 5.0 mmol), VTES (0.952 g, 5.0 mmol), MAA (0.430 g, 5.0 mmol) and the cross-linker DVB (0.163 g, 1.0 mmol) was added dropwise. The polymerization was performed with vigorous stirring for 24 h at 80 °C to form coated microspheres. The resultant coated microspheres were purified by centrifugation and washed first with water followed with *N*,*N*-dimethylformamide (DMF). Then, the coated microspheres were dispersed in DMF at 40 °C for 72 h to remove the core template. The elimination of the core template was judged by dropping the DMF solution into water until no turbidity or deposition could be seen. Lastly, the resultant PS-*co*-PAEMA-*co*-PVTES-*co*-PMAA hollow microspheres were purified by centrifugation and then dispersed in water for subsequent use.

**2.2.3 Preparation of the PS-*co*-PAEMA-*co*-PE-*co*-PMAA hollow shell–corona microspheres with a mesoporous shell.** Hydrochloric acid (37 wt%, 3.0 mL) was added to the aqueous dispersion of the PS-*co*-PAEMA-*co*-PVTES-*co*-PMAA hollow microspheres (100 mL, containing 3.65 g of the hollow microspheres), and then the dispersion was kept at room temperature for 24 h. The hollow microspheres were purified by centrifugation and then dispersed in aqueous hydrofluoric acid (100 mL, ~9 wt%) at room temperature for 24 h. The resultant PS-*co*-PAEMA-*co*-PE-*co*-PMAA hollow shell–corona microspheres with a mesoporous shell were purified by centrifugation, washed with water, and finally dispersed in water.

### 2.3 Encapsulation of alcohol within the microspheres

An aqueous dispersion of the PS-*co*-PAEMA-*co*-PE-*co*-PMAA microspheres (1.0 mL, containing $3.2 \times 10^{-2}$ g of the hollow microspheres) was added to a saturated aqueous solution of 1-phenylethanol ($6.0 \times 10^{-2}$ mmol mL$^{-1}$, 9.0 mL) at room temperature. After being stirred for 1 h, the mixture was filtered with a 0.20 μm filter and the concentration of 1-phenylethanol in the filtrate was measured by HPLC. The amount of 1-phenylethanol encapsulated within the microspheres was calculated from the difference between the fresh 1-phenylethanol aqueous solution and the filtrate. The volume percent $P$ occupied by the encapsulated 1-phenylethanol within the microcavity of the microspheres was calculated by the following equation:

$$P = \frac{m_a/\rho_a}{\left(m_b/\frac{4}{3}\pi(R^3 - r^3)\rho_c\right) \times \frac{4}{3}\pi\, r^3},$$

where $m_a$ and $m_b$ are the weight of the encapsulated 1-phenylethanol and the PS-*co*-PAEMA-*co*-PE-*co*-PMAA hollow shell–corona microspheres, $\rho_a$ and $\rho_c$ are the density of 1-phenylethanol and the wall of the hollow microspheres, $R$ and $r$ are the average radius of the hollow microspheres and the average radius of the microcavity, respectively. Herein, the density of the wall of the hollow shell–corona microspheres, $\rho_c$, is estimated to be approximately equal to that of the bulk polymer materials, 1 g cm$^{-3}$.

### 2.4 Preparation of microreactor by immobilization of Au nanoparticles on the microspheres

To a flask, an aqueous solution of $HAuCl_4$ (2.0 mmol L$^{-1}$, 25.0 mL) and an aqueous dispersion of the PS-*co*-PAEMA-*co*-PE-*co*-PMAA microspheres (15.0 mL, containing 0.25 g of the microspheres) were added. The mixture was stirred for 2 h, and then the pH adjusted to ~7 with 0.05 mol L$^{-1}$ aqueous NaOH. Subsequently, cold aqueous $NaBH_4$ (20.0 mmol L$^{-1}$, 10.0 mL) was slowly added with vigorous stirring. The final dispersion was adjusted to 100.0 mL with water, wherein the Au concentration is 0.50 mmol L$^{-1}$.

### 2.5 Catalyst testing

**2.5.1 Typical procedures for aerobic alcohol oxidation.** Alcohol (1.0 mmol), a suitable base (3.0 mmol), the aqueous dispersion of the microreactor (10.0 mL, containing

 

$5.0 \times 10^{-3}$ mmol Au catalyst), and a given volume of toluene (only under the biphasic conditions) were added to a 50 mL tube-like glass reactor equipped with a reflux condenser. The resulting mixture was stirred at 80 °C and the oxidation was carried out with bubbling $O_2$ (*ca.* 0.05 L $min^{-1}$) at atmospheric pressure. The progress of the oxidation was monitored by high performance liquid chromatography (HPLC).

**2.5.2 Catalyst recycling of the microreactor.** Oxidation of 1-phenylethanol under toluene–aqueous biphasic condition was chosen to evaluate the recycling of the microreactor. After the oxidation was completed (3 h), the organic phase was decanted and then analyzed with HPLC, then the same amounts of 1-phenylethanol (1.0 mmol) and toluene (2.0 mL) were added to the aqueous phase containing the microreactor, and the next run of oxidation was performed at 80 °C with bubbling of $O_2$ at atmospheric pressure for 3 h, under the same oxidation conditions as for the first run.

To detect the Au catalyst leaching into the organic phase, the organic phase containing the oxidation product (acetophenone) was analyzed by atomic absorption spectrum (AAS). To diagnose aggregation of the immobilized Au nanoparticles, the aqueous dispersion of the recycled microreactor was first characterized by UV-vis absorption spectroscopy and then by transmission electron microscopy (TEM). To check the stability of the PS-*co*-PAEMA-*co*-PE-*co*-PMAA hollow shell–corona microspheres in the catalytic oxidation, the aqueous dispersion of the recycled microreactor was first frozen in liquid nitrogen, freeze-dried to remove water, and then characterized by solid-state $^{13}C$ NMR.

**2.5.3 Lifetime of the microreactor.** To explore the lifetime of the microreactor, oxidation of 1-phenylethanol employing very dilute suspension of the microreactor at a molar ratio of substrate/Au of 10 000 : 1 was tested. To a 50 mL tube-like glass reactor equipped with a reflux condenser, 10.0 mL of aqueous dispersion of the microreactor containing $1.0 \times 10^{-3}$ mmol of Au catalyst, 30 mmol of KOH, 10.0 mmol of 1-phenylethanol and 2.0 mL of toluene were added. The oxidation at 80 °C was started by bubbling through $O_2$ (*ca.* 0.05 L $min^{-1}$) at atmospheric pressure, and the oxidation was monitored by HPLC.

### 2.6 General characterizations

TEM was conducted by using a Philips T20ST electron microscope at an acceleration voltage of 200 kV, whereby a small drop of the colloidal dispersion was deposited onto a piece of copper grid and dried at room temperature under atmospheric pressure. Fourier-transform infrared spectra (FTIR) were determined on a Bio-Rad FTS 135 spectrometer on a potassium bromide pellet and the diffuse reflectance spectra were scanned over the range 400–4000 $cm^{-1}$. The solid-state $^{13}C$ NMR measurements were performed on a Varian Infinityplus wide-bore (89 mm) NMR spectrometer at spin rate of 13 kHz, which was equipped with a double-resonance HX CP/MAS probe. HPLC analysis was performed on a LabAlliance PC2001 system equipped with a C18 column and a UV-vis detector using a mixture of $CH_3CN$ and water (6 : 4 by volume) as eluent. The nitrogen adsorption was performed on a Micromeritics Gemini V system at 77 K. The UV-vis absorption spectra were recorded on a TU-8110 UV-vis spectrophotometer at 25 °C. AAS analysis was performed on a Solaar AAS 2 atomic absorption spectrometer.

## 3. Results and discussion

### 3.1 Synthesis and characterization of hollow shell–corona microspheres with a mesoporous shell

The microspheres synthesized are composed of three parts: (1) a hydrophilic corona of PMAA, which keeps the microspheres suspended in aqueous solution; (2) a chelating mesoporous shell of PS-*co*-PAEMA-*co*-PE, in which the chelate segment of PAEMA is used to immobilize the Au nanoparticles (the PS segment is introduced to increase the thermal stability of the hollow microspheres, since the glass transition temperature ($T_g$) of the PAEMA segment is very low (~3 °C),[18] and the PE segment results from the hydrolysis of the PVTES segment to produce the mesopore in the shell); and (3) a hydrophobic microcavity to encapsulate and concentrate the alcohol during catalysis.

Fig. 2 shows the synthesis of the microspheres. Firstly, the core template of PS-*co*-PMAA microspheres is synthesized by one-stage soap-free polymerization as described elsewhere.[15] Subsequently, polymerization of styrene, AEMA, VTES and MAA in the presence of the DVB cross-linker on the sacrificial template of the PS-*co*-PMAA microspheres forms coated microspheres of PS-*co*-PMAA/PS-*co*-PAEMA-*co*-PVTES-*co*-PMAA. Then the coated microspheres are dispersed in DMF to remove the core template, producing hollow shell–corona microspheres of PS-*co*-PAEMA-*co*-PVTES-*co*-PMAA. These are then dispersed in aqueous HCl, in which the shell-forming segment of PVTES is hydrolyzed to form siloxanes, and then the resultant siloxane component is removed with hydrofluoric acid to form mesopores in the shell, producing PS-*co*-PAEMA-*co*-PE-*co*-PMAA hollow shell–corona microspheres with a mesoporous shell. It should be pointed out that PVTES is easily hydrolyzed both in acidic and basic aqueous solution.[19–21] Herein, mesopores are introduced into the shell of the microspheres through hydrolysis of the PVTES segment in aqueous acid, which is useful to avoid ionization of the PMAA corona in basic aqueous solution. It is believed that the mesopores randomly locate in the shell-layer as shown in Fig. 1, since the mesopores result from the hydrolysis of the random copolymer of PS-*co*-PAEMA-*co*-PVTES.

It is found that the coating monomers of styrene, AEMA, VTES, MAA and the cross-linker DVB are almost quantitatively converted to the coated microspheres. After the subsequent removal of the core template and the hydrolysis of the PVTES segment, the weight of the resultant PS-*co*-PAEMA-*co*-PE-*co*-PMAA hollow shell–corona microspheres with a mesoporous shell is about 59 wt% of the coated microspheres.

Fig. 3 shows the TEM images taken during the synthesis of the microspheres. Fig. 3A shows the core template of the microspheres (average diameter ~230 nm), Fig. 3B shows the coated microspheres (average diameter ~330 nm), and Fig. 3C shows the hollow microspheres (average diameter

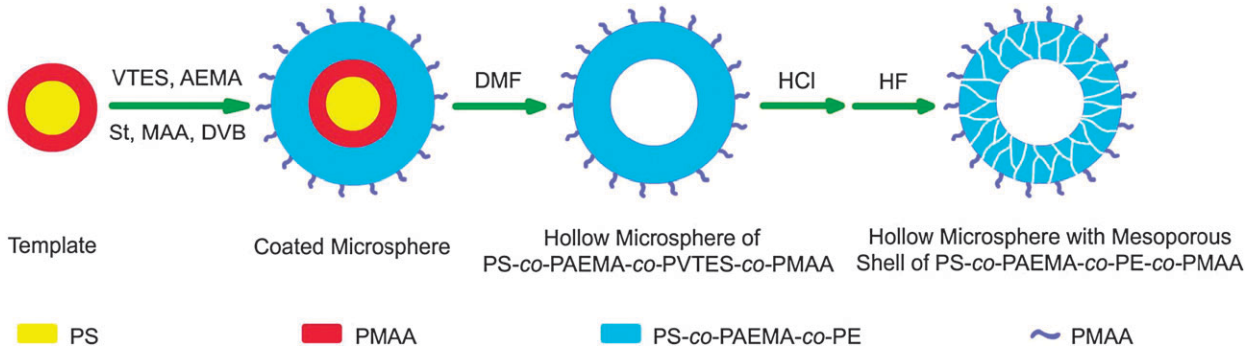


**Fig. 2** Synthesis of the PS-*co*-PAEMA-*co*-PE-*co*-PMAA microspheres.



~320 nm, average wall thickness ~52 nm, extent of microcavity ~210 nm). Clearly, the size of the PS-*co*-PAEMA-*co*-PVTES-*co*-PMAA hollow microspheres is a little smaller than that of the coated microspheres, indicating a slight shrinkage of the coating materials during dissolution of the core template. In addition, we also observed something within the hollow microspheres; we think that some of the coating monomers diffuse into the swollen core template of the PS-*co*-PMAA microspheres, and that these polymerize in the presence of the cross-linker DVB to form insoluble polymeric materials. Fig. 3D shows the microspheres with a mesoporous shell, and indicates that their size, ~310 nm, is almost as same as those of the hollow microspheres (Fig. 3C), while the wall thickness, ~50 nm, is slightly smaller.

To confirm formation of mesoporous structure in the shell, the dried PS-*co*-PAEMA-*co*-PE-*co*-PMAA hollow shell–corona microspheres were further characterized by nitrogen adsorption. Fig. 4A shows their $N_2$ isotherms at 77 K, from which the distribution of the pore size is calculated using the Barrett–Joyner–Halenda (BJH) method. As shown in Fig. 4B, the shape of the $N_2$ isotherms corresponds to a mesoporous material with pore size distribution centered at 2 nm. Here it should be pointed out that the average size of the mesopores in aqueous solution should be larger than 2 nm, since the PS-*co*-PAEMA-*co*-PE-*co*-PMAA hollow shell–corona microspheres become swollen in aqueous solution due to the hydrophilic PMAA corona.

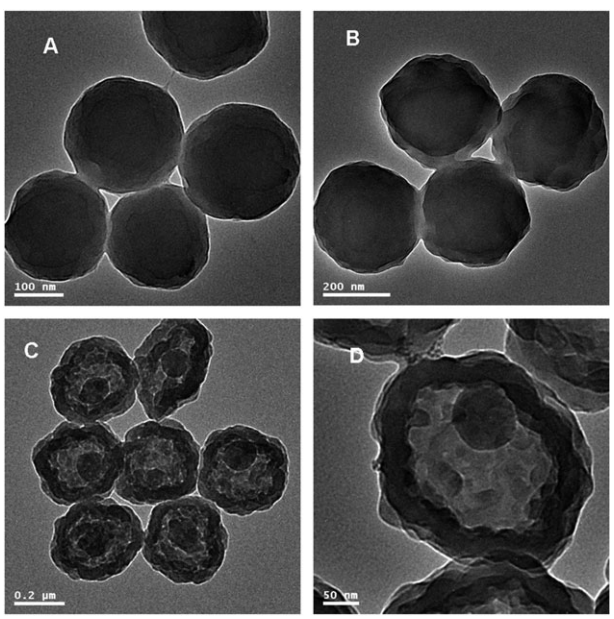


**Fig. 3** TEM images of (A) the core template of the PS-*co*-PMAA microspheres, (B) the microspheres coated with PS-*co*-PMAA/PS-*co*-PAEMA-*co*-PVTES-*co*-PMAA, (C) the hollow microspheres coated with a mesoporous shell of PS-*co*-PAEMA-*co*-PVTES-*co*-PMAA, and (D) the hollow shell–corona microspheres with a mesoporous shell of PS-*co*-PAEMA-*co*-PE-*co*-PMAA.

Fig. 5 shows the solid-state $^{13}C$ CPMAS NMR spectra taken during the synthesis of the microspheres. Lines A, B, C and D are the spectra of the core template of the PS-*co*-PMAA microspheres, the coated microspheres of PS-*co*-PMAA/PS-*co*-PAEMA-*co*-PVTES-*co*-PMAA, the PS-*co*-PAEMA-*co*-PVTES-*co*-PMAA hollow microspheres and the PS-*co*-PAEMA-*co*-PE-*co*-PMAA hollow shell–corona microspheres with a mesoporous shell, respectively. Comparing spectrum C with spectrum B, the relative intensities in chemical shift of 127 ppm and 40 ppm are weakened, suggesting removal of the core of PS-*co*-PMAA microspheres and formation of hollow microspheres. In addition, as indicated by the insets above spectrum C, the characteristic chemical shifts due to the corresponding carbons are present, which further conforms their constitution, and this is also confirmed by FTIR (Fig. S1†).

### 3.2 Encapsulation of alcohol within the microspheres

Due to the hydrophilic PMAA corona, the microspheres can be easily dispersed (and remain suspended) in aqueous solution. It is found that, similar to other polymeric capsules,[22–24] these microspheres can encapsulate and concentrate guest organic molecules. Here, we encapsulate a hydrophobic alcohol (1-phenylethanol) by way of example. After addition of the microspheres into a saturated aqueous solution of 1-phenylethanol at room temperature, we found that the concentration of 1-phenylethanol within the hollow microspheres was almost 389 times higher than those in water, the encapsulated 1-phenylethanol taking up 100% of microcavity space. We point out that the percentage of the encapsulated guest molecules is estimated by the extent of the microcavity measured with TEM, and so this should be a little higher than the actual value, since the microspheres will become swollen in aqueous solution due to the hydrophilic PMAA corona. As shown in Fig. 2, the microspheres contain a hydrophilic corona and a hydrophobic shell, and therefore we think that the microenvironment in the microcavity of the hollow microspheres is

 

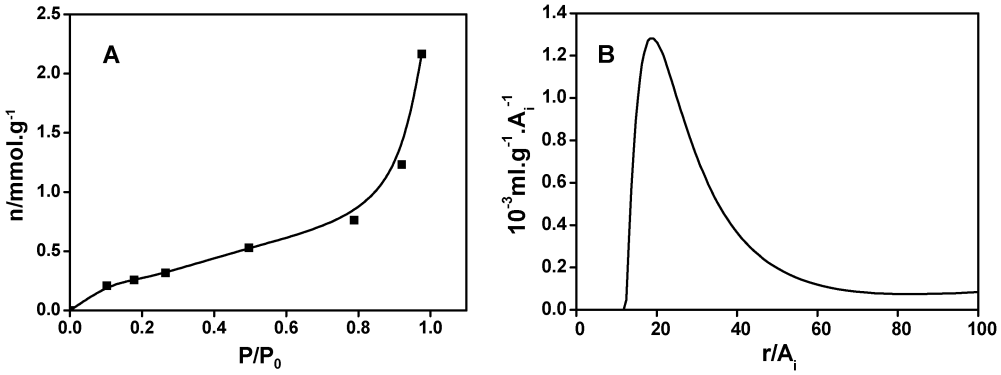


**Fig. 4** (A) $N_2$ isotherms of the hollow shell–corona microspheres with a mesoporous shell at 77 K, and (B) the size distribution of the mesopores.



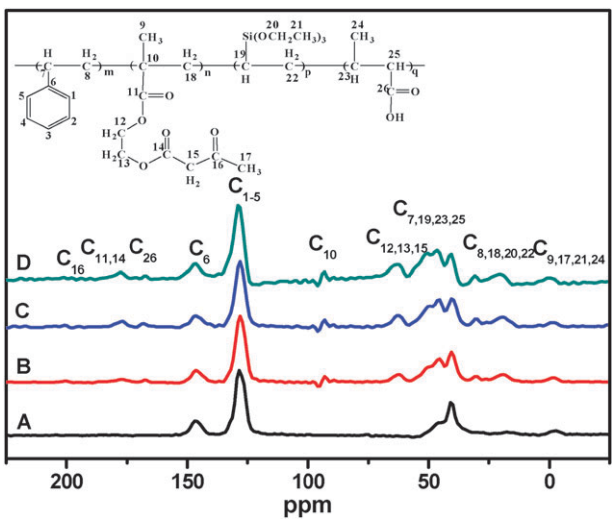


**Fig. 5** $^{13}C$ CPMAS NMR spectra of (A) the core template of the PS-*co*-PMAA microspheres, (B) the microspheres coated with PS-*co*-PMAA/PS-*co*-PAEMA-*co*-PVTES-*co*-PMAA, (C) the hollow microspheres coated with a mesoporous shell of PS-*co*-PAEMA-*co*-PVTES-*co*-PMAA, and (D) the hollow shell–corona microspheres with a mesoporous shell of PS-*co*-PAEMA-*co*-PE-*co*-PMAA.

generally hydrophobic. Thus, the encapsulation of 1-phenylethanol is mainly ascribed to the hydrophobic microenvironment provided by the microspheres.

### 3.3 Preparation of microreactor by immobilization of Au nanoparticles on the microspheres

Since the PAEMA segment provides the chelate ligands of the β-diketone for coordination with metal precursors,[18,25] polymeric materials containing the PAEMA segment can be used to immobilize metal catalysts. We have successfully immobilized Pd nanoparticle catalysts on PAEMA-based polymers and studied their applications for the C–C coupling reaction and hydrogenation.[14,26] In the current work, we found that Au nanoparticles can be easily immobilized on the microspheres. When $HAuCl_4$ was added to the aqueous dispersion of the microspheres, Au ions were coordinated with the chelate ligands in the PAEMA segment, and subsequently reduced by aqueous $NaBH_4$, which resulted in the formation of Au nanoparticles immobilized on the hollow microspheres. Fig. 6 shows the TEM image of the resultant microreactor and the size distribution of the immobilized Au nanoparticles. It can clearly be seen that the Au nanoparticles are uniformly dispersed on the hollow microspheres, and that the average size of the Au nanoparticles is 5.1 nm. Thus, we deduce that the Au nanoparticles are selectively embedded mainly on the shell-layer, since the chelate segment of PAEMA is primarily located in the shell of the microspheres. Furthermore, the Au nanoparticles are believed to be outside the mesopores (as shown in Fig. 1), since they are larger than the mesopores.

It is well documented that UV-vis spectroscopy can be used to diagnose the aggregation state of Au nanoparticles.[27,28] For example, highly dispersed 5–20 nm Au nanoparticles exhibit an absorbance peak at ~520 nm.[27] As the gold particle size decreases, a hypsochromic shift of the characteristic absorbance occurs, and no sharp absorbance peak is observed within the UV-vis range when the size of gold nanoparticles falls below 3 nm.[28] Fig. 7 shows the UV-vis absorption spectra of an aqueous dispersion of the microreactors, in which a distinct absorption peak around 520 nm is clearly observed, indicating formation of ~5 nm Au nanoparticles.

Similarly to the PS-*co*-PAEMA-*co*-PE-*co*-PMAA hollow shell–corona microspheres themselves, the microreactors can also be easily dispersed in aqueous solution due to the hydrophilic PMAA corona, suggesting that they are a quasi-homogeneous catalyst. In addition, we also found that the microreactor is selectively dispersed in the aqueous phase (as shown by the insets in Fig. 7) when a hydrophobic solvent such as toluene is added into the aqueous dispersion. This feature makes the microreactor especially suitable for organic–aqueous biphasic catalysis, as discussed later.

### 3.4 Aerobic alcohol oxidation

The oxidation of alcohols to aldehydes or ketones is a pivotal functional group transformation in organic chemistry.[29–31] Recently, aerobic alcohol oxidation has attracted much interest, and various Au catalysts immobilized on inorganic materials[32–36] and polymers[37–41] have been investigated as potential catalysts. It was concluded that the oxidation follows the Langmuir–Hinselwood reaction mechanism, that is, the higher concentration of the reactants in a confined region, the faster the oxidation.[42] As discussed above, the present hollow shell–corona microspheres with a mesoporous shell can encapsulate and concentrate alcohols in water. Therefore,

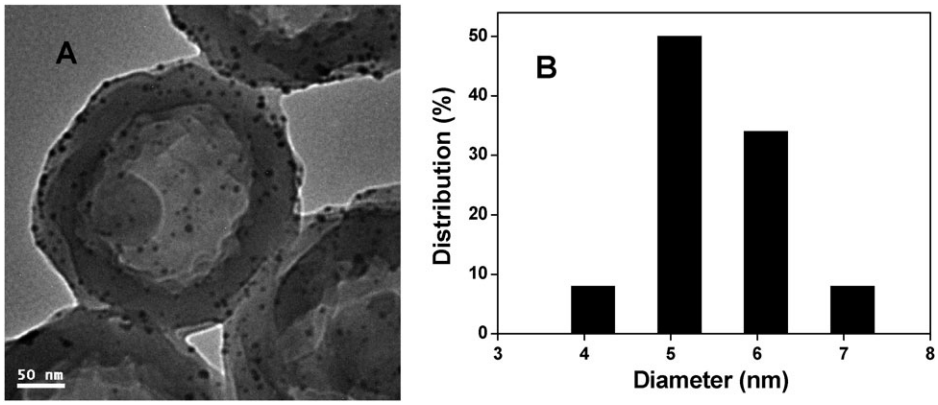


**Fig. 6** (A) TEM image of the microreactors, and (B) the size distribution of the immobilized Au nanoparticles.

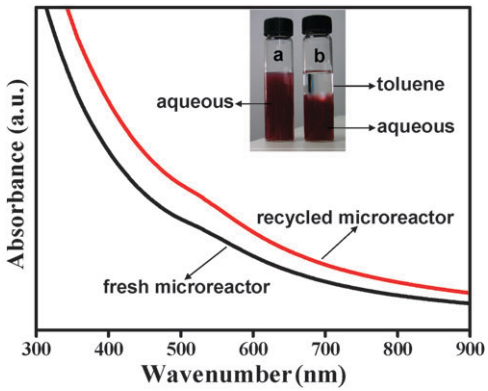


**Fig. 7** The UV-vis spectra of the aqueous dispersion of the fresh and recycled microreactor. Insets: optical images of the aqueous dispersion of the microreactor.

aerobic alcohol oxidation within the present microreactor is expected to be efficient due to concentrated reactants.

By way of example, we studied the aerobic oxidation of 1-phenylethanol within the present microreactor in aqueous phase and under toluene–aqueous biphasic conditions. As shown in Fig. 8A, in aqueous solution, alcohol is trapped in the hollow shell–corona microspheres through the mesoporous shell due to the hydrophobic microenvironment, and oxidation of alcohol with concentrated reactants occurs by the action of the Au nanoparticles. During the oxidation, the product (acetophenone) accumulates within the microreactor and gradually diffuses into the aqueous phase through the mesoporous shell. Clearly, there exists an alcohol–ketone dispersion balance between the water and within the microreactor. Under the toluene–aqueous biphasic conditions, the alcohol toluene solution forms one phase, while water (containing the microreactor) forms the other. The alcohol and toluene molecules first diffuse into the water and are then encapsulated in the microreactor, within which oxidation takes place. The product then diffuses into the water and is extracted into the organic phase.

One would expect there to be a balance of reactants between the toluene solution, aqueous solution, and the microreactors. Clearly, compared with oxidation performed in aqueous phase, oxidation performed under toluene–aqueous biphasic conditions has a disadvantage that the alcohol confined within the microreactor is diluted by toluene, but meanwhile it has an advantage that the diffusion of the oxidation product out of the microreactor can be accelerated by extraction due to the toluene phase, as shown in Fig. 8. It is found that the oxidation under biphasic conditions is most efficient at a toluene–water volume ratio of 1 : 5 (Fig. S2).

Fig. 9 shows the dependence of yield of acetophenone with respect to time during the alcohol oxidation performed in aqueous phase and under toluene–aqueous biphasic conditions, employing the optimized base KOH (Fig. S3). Clearly, an almost quantitative yield of acetophenone is achieved in 2 h at 80 °C employing the optimized base, whether the oxidation is performed in the aqueous phase or under toluene–aqueous biphasic conditions. However, the initial oxidation under toluene–aqueous biphasic conditions is faster than in the aqueous phase, which affords a higher turnover frequency (TOF) value (667 $h^{-1}$ *vs.* 317 $h^{-1}$, as calculated by the number of Au atoms after the first 5 min).

To evaluate the effect of the mesopores or permeability of the microreactor on alcohol oxidation, a reference microreactor of Au nanoparticles immobilized hollow shell–corona microspheres of PS-*co*-PAEMA-*co*-PAM is synthesized (Fig. S4). These are the same as the microreactors discussed earlier, but they have no mesopores in the shell layer.[14] The size of the Au nanoparticles immobilized on the reference microreactor, 5.7 nm, is very close to those on the microporous microreactors. Fig. 10 shows the dependence of yield of acetophenone with respect to time during the alcohol oxidation performed in aqueous phase and under toluene–aqueous biphasic conditions employing the present microreactor and the reference microreactor, respectively. The result indicates that the microreactors with a mesoporous shell are much more efficient than the reference microreactor under aqueous condition. However, under toluene–aqueous biphasic conditions, the microreactor is as efficient as the reference microreactor. The reason for this is possibly due to the faster diffusion of acetophenone (due to the mesoporous shell) out of the microporous microreactor compared to the reference microreactor, when under aqueous conditions. However, under biphasic conditions, the diffused acetophenone is quickly extracted into the organic phase, and the diffusion is accelerated whether the microreactor has a mesoporous shell or not, and therefore the two microreactors have similar catalytic efficiency.

 

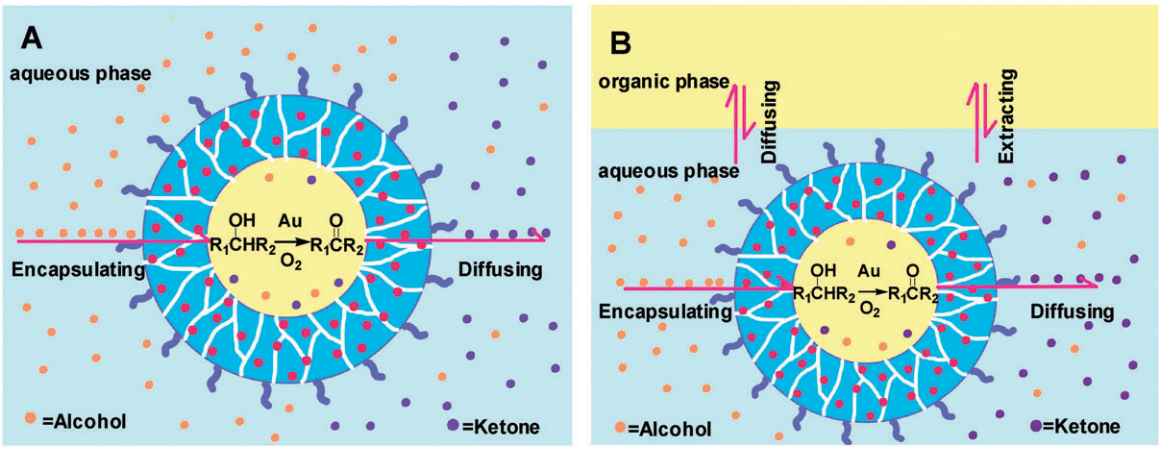


**Fig. 8** Alcohol oxidation within the microreactor (A) in the aqueous phase and (B) under toluene–aqueous biphasic conditions.

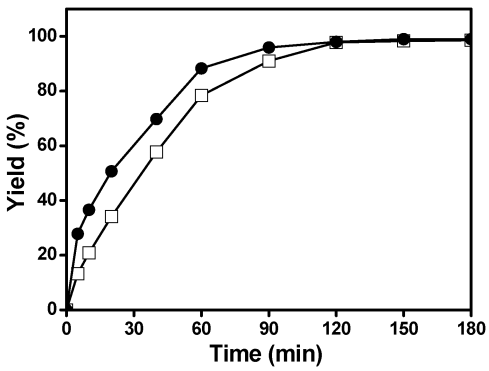


**Fig. 9** The dependence of yield of acetophenone with respect to time during the alcohol oxidation performed in aqueous phase (□) and under toluene–aqueous biphasic conditions (●). *Reaction conditions*: 10.0 mL of aqueous dispersion of the microreactor containing $5.0 \times 10^{-3}$ mmol of Au catalyst, 1.0 mmol of 1-phenylethanol, 3.0 mmol of KOH, 2.0 mL of toluene (only under organic–aqueous biphasic conditions), bubbling $O_2$ at 0.05 L $min^{-1}$, 80 °C, HPLC yield.

Up to now, several Au nanocatalysts immobilized on or stabilized with polymeric materials such as microgel,[39] polystyrene (PS),[40] and dimethylamino-functionalized resin (DMA-resin)[41] have been proposed for aerobic alcohol oxidation. Compared with the Microgel-Au or Au/DMA-resin catalyst, the present microreactor affords a competitive TOF value (Table 1, entries 1–4). We found that aerobic oxidation of 1-phenylethanol within the microporous microreactor at 25 °C proceeds with a slightly lower TOF value than for the Au/PS catalyst (Table 1, entries 5–6). However, it should be pointed out that various parameters such as the size of Au nanoparticles,[38] the nature of the support,[43] and the dissolution of $O_2$ in the reaction mixture[44] can affect the catalytic activity of Au nanocatalyst for aerobic alcohol oxidation.

To further evaluate the microreactor, aerobic oxidations of several typical alcohols within the microreactor under organic–aqueous biphasic conditions were explored. For the secondary alcohols that have either an electron-deficient or electron-rich *para*-substituent, such as 1-phenylethanol, 1-(4-methoxyphenyl)ethanol, 1-(4-methylphenyl)ethanol, 1-(4-chlorophenyl)-ethanol and benzhydrol, the oxidation within the microreactor runs efficiently, almost quantitative yields are achieved in 30–120 min, and the microreactor affords a TOF ranging from 100 to 400 $h^{-1}$ (Table 2, entries 1–5). In contrast, the oxidation of 1-(2-methylphenyl)ethanol within the microreactor is less efficient, possibly due to the steric hindrance of the *meta*-substituent (Table 2, entry 6), and above 99% yield is achieved when the oxidation extends to a relatively long time

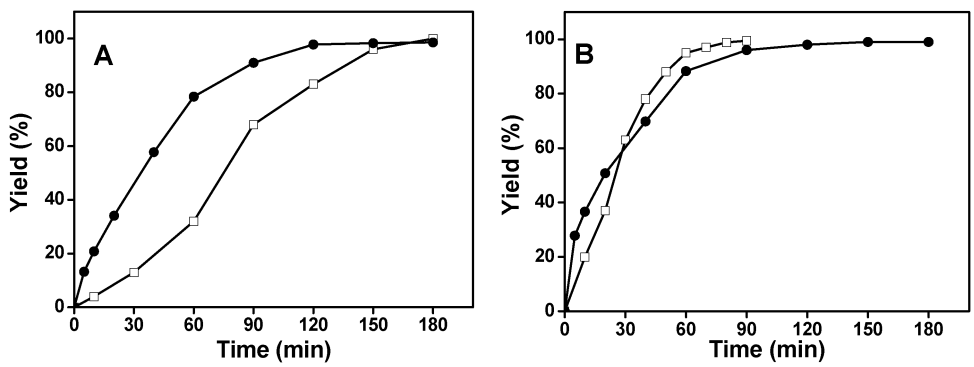


**Fig. 10** The dependence of yield on time in the oxidation of 1-phenylethanol performed within the microporous microreactor (●) and the reference microreactor (□), (A) in aqueous solution and (B) under toluene–aqueous biphasic conditions. *Reaction conditions*: 10.0 mL of aqueous dispersion of microreactor containing $5.0 \times 10^{-3}$ mmol of Au catalyst, 3.0 mmol of KOH, 1.0 mmol of 1-phenylethanol, 2.0 mL of toluene (only under organic–aqueous biphasic conditions), bubbling $O_2$ at 0.05 L $min^{-1}$, 80 °C, HPLC yield.

**Table 1** Aerobic alcohol oxidation employing different immobilized noble-metal nanocatalysts

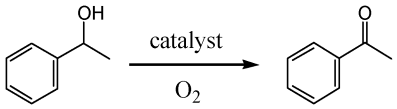


| Entry | Catalyst | Conditions | Yield (%) | TOF ($h^{-1}$)[b] |
|---|---|---|---|---|
| 1[a] | Microreactor (this work) | 80 °C, $H_2O$–toluene, KOH, bubbling $O_2$, 0.50 mol% catalyst, 2 h | 98 | 100 [200[c]] |
| 2[a] | Microreactor (this work) | 80 °C, $H_2O$, KOH, bubbling $O_2$, 0.50 mol% catalyst, 2 h | 98 | 100 [160[c]] |
| 3[d] | Microgel-Au | 60 °C, $H_2O$, NaOH, 1.5 atm $O_2$, 0.2 mol% catalyst, 1 h | 75 | 375 |
| 4[e] | Au/DMA-resin | 60 °C, EtOH–$H_2O$, KOH, 5 atm $O_2$, 0.5 mol% catalyst | — | 120 |
| 5[a] | Microreactor (this work) | 25 °C, $H_2O$–toluene, KOH, bubbling $O_2$, 1.0 mol% catalyst, 3 h | 60 | 20 |
| 6[f] | Au/PS | Room temperature, 1 atm $O_2$, benzotrifluoride–$H_2O$, 1 mol% catalyst, 3 h | 96 | 32 |

[a] See the Experimental section for details. [b] TOF calculated from the total number of Au atoms at the end of the reaction. [c] TOF calculated by the total Au atoms at 75% yield. [d] Reference catalyst in ref. 40. [e] Reference catalyst in ref. 41. [f] Reference catalyst in ref. 42.



**Table 2** Aerobic alcohol oxidation within the microreactor under organic–aqueous biphasic conditions[a]

| Entry | Alcohol | Product | Time (min) | Yield[b] (%) | TOF[c] ($h^{-1}$) |
|---|---|---|---|---|---|
| 1 | 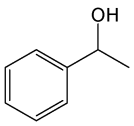 | 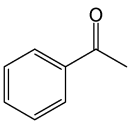 | 120 | 98 | 100 |
| 2 | 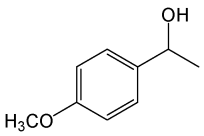 | 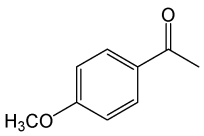 | 60 | > 99 | 200 |
| 3 | 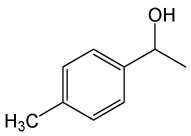 | 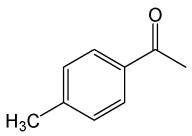 | 30 | > 99 | 400 |
| 4 | 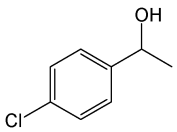 | 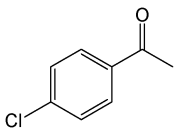 | 60 | > 99 | 200 |
| 5 | 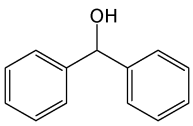 | 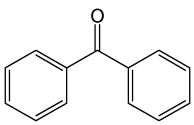 | 30 | > 99 | 400 |
| 6 | 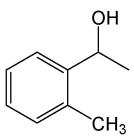 | 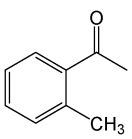 | 780 | > 99 | 15 |
| 7[d] | 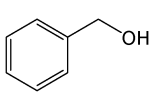 | 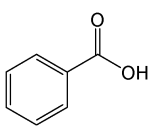 | 105 | > 99 | 110 |

[a] See the reaction conditions indicated in the Experimental section. [b] HPLC or $^1$HNMR yield. [c] TOF is measured based on total Au atoms at the end of the oxidation. [d] The oxidation is performed in aqueous solution.

 

of 780 min. The aerobic oxidation of a typical primary alcohol of benzyl alcohol within the microreactor in aqueous solution is also studied and the microreactor affords a moderate TOF of 110 $h^{-1}$ (Table 2, entry 7). It is found that benzaldehyde is first formed, and then this is further oxidized into benzoic acid. It should be pointed out that the oxidation of benzyl alcohol is performed in aqueous solution instead of under organic–aqueous biphasic conditions, since the oxidation product (benzoic acid) is easily soluble in water. For aliphatic alcohols such as cyclohexanol, the oxidation within the microreactor runs inefficiently, similarly to those employing general Au nanocatalysts.[39–41]

The recycling of the microreactors and leaching of Au nanocatalyst were checked using the oxidation of 1-phenylethanol under toluene–aqueous biphasic conditions at 80 °C as a typical example. After the oxidation was just complete (3 h), the organic phase was removed by simple decantation and 1-phenylethanol was reloaded. We found that the microreactors can be recycled at least 6 times without losing activity. AAS analysis of the organic phase indicates that the Au catalyst leaching into organic phase can be ignored. In addition, no aggregation of the immobilized Au nanoparticles was confirmed by UV-vis measurements (Fig. 7) or TEM observations (Fig. 11), which shows that the average size of the Au nanoparticles in the recycled microreactor, 5.3 nm, is very similar to those in the fresh microreactor.

Furthermore, from the TEM image of the recycled microreactor (Fig. 11), it is clearly observed that the size and morphology of the hollow shell–corona microspheres are almost unchanged after 6 cycles of oxidation. This is ascribed to the fact that the PS-*co*-PAEMA-*co*-PE-*co*-PMAA hollow microspheres are cross-linked by 4 mol% DVB (see Experimental section), which makes the hollow microspheres stable. $^{13}C$ CPMAS NMR analysis of the recycled microreactor further suggests that the hollow microspheres in the recycled microreactor have a similar composition to the fresh PS-*co*-PAEMA-*co*-PE-*co*-PMAA hollow microspheres (Fig. S5). All these results confirm the stability of the PS-*co*-PAEMA-*co*-PE-*co*-PMAA hollow microspheres and the reusability of the present microreactor.

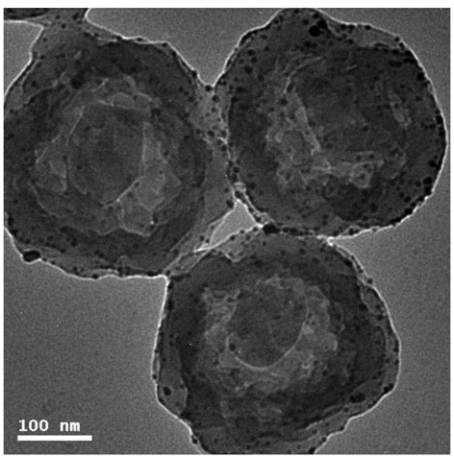


**Fig. 11** TEM image of the recycled microreactor after 6 cycles of oxidation under organic–aqueous biphasic conditions.

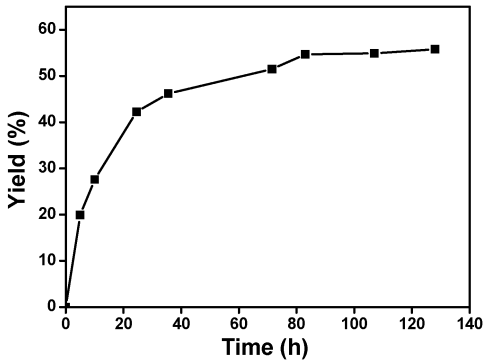


**Fig. 12** The dependence of yield on time in the oxidation of 1-phenylethanol under toluene–aqueous biphasic conditions for the microreactor endurance testing. *Reaction conditions*: 10.0 mL of aqueous dispersion of the microreactor containing $1.0 \times 10^{-3}$ mmol of Au catalyst, 30 mmol of KOH, 10.0 mmol of 1-phenylethanol, 2.0 mL of toluene, bubbling $O_2$ at 0.05 L $min^{-1}$, 80 °C, HPLC yield.

The lifetime or endurance of the present microreactor was also tested by greatly diluting the microreactors in alcohol (molar ratio of alcohol–Au catalyst of 10 000 : 1). As shown in Fig. 12, the microreactor can be used for 80 h at least under the present alcohol oxidation.

## 4. Conclusions

Shell–corona hollow microspheres with a mesoporous shell of PS-*co*-PAEMA-*co*-PE-*co*-PMAA have been synthesized. They contain a hydrophilic corona of PMAA to keep the hollow microspheres suspended in aqueous solution, and a mesoporous chelating shell to immobilize the Au nanocatalyst and to increase the permeability of the microreactor. The hollow shell–corona microspheres can encapsulate organic molecules such as 1-phenylethanol, and it is found that the concentration of 1-phenylethanol within the microspheres is much higher than in water. The catalyst (5.1 nm Au nanoparticles) is immobilized on the microspheres, and the resulting microreactor is demonstrated to be efficiently catalyze the aerobic oxidation of alcohols under quasi-homogeneous aqueous solution and under organic–aqueous biphasic conditions. Other benefits of the microreactor include easy catalyst reuse, low catalyst leaching and long-term stability. We anticipate that the present microreactor has promising potential in catalysis.

## Acknowledgements

The financial support by National Science Foundation of China (No. 20974051), Tianjin Natural Science Foundation (No. 09JCYBJC02800), and the Program for New Century Excellent Talents in University (No. NCET-06-0216) is gratefully acknowledged.

## References

1 D. M. Vriezema, M. C. Aragonès, J. A. A. W. Elemans, J. J. L. M. Cornelissen, A. E. Rowan and R. J. M. Nolte, *Chem. Rev.*, 2005, **105**, 1445–1490.
2 S. M. Leeder and M. R. Gagné, *J. Am. Chem. Soc.*, 2003, **125**, 9048–9054.

3 X. Huang, C. Guo, J. Zuo, N. Zheng and G. D. Stucky, *Small*, 2009, **5**, 361–365.
4 J. Gao, G. Liang, B. Zhang, Y. Kuang, X. Zhang and B. Xu, *J. Am. Chem. Soc*., 2007, **129**, 1428–1433.
5 J. Li and H. Zeng, *Angew. Chem., Int. Ed*., 2005, **44**, 4342–4345.
6 M. Nallani, H.-P. M. de Hoog, J. J. L. M. Cornelissen, A. R. A. Palmans, J. C. M. van Hest and R. J. M. Nolte, *Biomacromolecules*, 2007, **8**, 3723–3728.
7 S. F. M. van Dongen, M. Nallani, J. J. L. M. Cornelissen, R. J. M. Nolte and J. C. M. van Hest, *Chem. Eur. J*., 2009, **15**, 1107–1114.
8 S. M. Kuiper, M. Nallani, D. M. Vriezema, J. J. L. M. Cornelissen, J. C. M. van Hest, R. J. M. Nolte and A. E. Rowan, *Org. Biomol. Chem*., 2008, **6**, 4315–4318.
9 S. Miao, C. Zhang, Z. Liu, B. Han, Y. Xie, S. Ding and Z. Yang, *J. Phys. Chem. C*, 2008, **112**, 774–780.
10 D. G. Shchukin and H. Möhwald, *Langmuir*, 2005, **21**, 5582–5587.
11 L. Lu and A. Eychmuller, *Acc. Chem. Res*., 2008, **41**, 244–253.
12 P.-A. Monnard, *J. Membr. Biol*., 2003, **191**, 87–97.
13 C. Nardin, S. Thoeni, J. Widmer, M. Winterhalter and W. Meier, *Chem. Commun*., 2000, 1433–1434.
14 Y. Lan, M. Zhang, W. Zhang and L. Yang, *Chem. Eur. J*., 2009, **15**, 3670–3673.
15 F. Wen, W. Zhang, P. Zheng, X. Zhang, X. Yang, Y. Wang, X. Jiang, G. Wei and L. Shi, *J. Polym. Sci., Part A: Polym. Chem*., 2008, **46**, 1192–1202.
16 X. Xu and S. A. Asher, *J. Am. Chem. Soc*., 2004, **126**, 7940–7945.
17 G. Li and X. Yang, *J. Phys. Chem. B*, 2007, **111**, 12781–12786.
18 T. Krasia, R. Soula, H. G. Börner and H. Schlaad, *Chem. Commun*., 2003, **538–539**.
19 K. A. Smith, *J. Org. Chem*., 1986, **51**, 3827–3830.
20 J. Li, J. Shi, C. Wei, P. Jiang, W. Huang and D. Zhuang, *J. Phys. Chem. C*, 2008, **112**, 13754–13762.
21 K. F. Ni, N. Sheibat-Othman, G. R. Shan, G. Fevotte and E. Bourgeat-Lami, *Macromolecules*, 2005, **38**, 9100–9109.
22 W. Meier, *Chem. Soc. Rev*., 2000, **29**, 295–303.
23 S. M. Marinakos, M. F. Anderson, J. A. Ryan, L. D. Martin and D. L. Feldheim, *J. Phys. Chem. B*, 2001, **105**, 8872–8876.
24 R. Ghan, T. Shutava, A. Patel, V. T. John and Y. Lvov, *Macromolecules*, 2004, **37**, 4519–4524.
25 T. Kaliyappan and P. Kannan, *Prog. Polym. Sci*., 2000, **25**, 343–370.
26 P. Zheng and W. Zhang, *J. Catal*., 2007, **250**, 324–330.
27 P. B. Johnson and R. W. Christy, *Phys. Rev. B: Solid State*, 1972, **6**, 4370–4379.
28 A. C. Templeton, J. J. Pietron, R. W. Murray and P. Mulvaney, *J. Phys. Chem. B*, 2000, **104**, 564–570.
29 G. J. Hutchings, *Chem. Commun*., 2008, 1148–1164.
30 T. Mallat and A. Baiker, *Chem. Rev*., 2004, **104**, 3037–3058.
31 B. Zhan and A. Thompson, *Tetrahedron*, 2004, **60**, 2917–2935.
32 A. Abad, P. Concepción, A. Corma and H. García, *Angew. Chem., Int. Ed*., 2005, **44**, 4066–4069.
33 A. Abad, C. Almela, A. Corma and H. García, *Tetrahedron*, 2006, **62**, 6666–6672.
34 P. Haider and A. Baiker, *J. Catal*., 2007, **248**, 175–187.
35 D. I. Enache, D. W. Knight and G. J. Hutchings, *Catal. Lett*., 2005, **103**, 43–52.
36 F.-Z. Su, Y.-M. Liu, L.-C. Wang, Y. Cao, H.-Y. He and K.-N. Fan, *Angew. Chem., Int. Ed*., 2008, **47**, 334–337.
37 S. Kanaoka, N. Yagi, Y. Fukuyama, S. Aoshima, H. Tsunoyama, T. Tsukuda and H. Sakurai, *J. Am. Chem. Soc*., 2007, **129**, 12060–12061.
38 H. Tsunoyama, H. Sakurai, Y. Negishi and T. Tsukuda, *J. Am. Chem. Soc*., 2005, **127**, 9374–9375.
39 A. Biffis, S. Cunial, P. Spontoni and L. Prati, *J. Catal*., 2007, **251**, 1–6.
40 H. Miyamura, R. Matsubara, Y. Miyazaki and S. Kobayashi, *Angew. Chem., Int. Ed*., 2007, **46**, 4151–4154.
41 T. Ishida, S. Okamoto, R. Makiyama and M. Haruta, *Appl. Catal., A*, 2009, **353**, 243–248.
42 A. Abad, A. Corma and H. Garcia, *Chem. Eur. J*., 2008, **14**, 212–222.
43 (*a*) F.-Z. Su, M. Chen, L.-C. Wang, X.-S. Huang, Y.-M. Liu, Y. Cao, H.-Y. He and K.-N. Fan, *Catal. Commun*., 2008, **9**, 1027–1032; (*b*) B. Jørgensen, S. E. Christiansen and M. L. D. Thomsen, *J. Catal*., 2007, **251**, 332–337.
44 Z. Hou, N. Theyssen, A. Brinkmann and W. Leitner, *Angew. Chem., Int. Ed*., 2005, **44**, 1346–1349.




 